3D SIMULATION OF THE MELTING DURING AN INDUSTRIAL SCALE ELECTRO-SLAG REMELTING PROCESS

A. Kharicha[1, 2], A. Ludwig[2], M.Wu[2]
(1) CD-Laboratory for Multi-Phase Modelling of Metallurgical Processes
(2) University of Leoben,
Franz-Joseph Strasse 18. 8700 Leoben, AUSTRIA,
abdellah.kharicha@uni-leoben.at

Keywords: Melting, Electroslag, droplet formation, MHD, Joule Heating, Simulations

Abstract

In the present paper, the droplet formation during melting of a 420 mm diameter flat electrode is simulated with an advanced three dimensional multiphase-Magneto-hydrodynamic numerical model. The momentum, energy and electromagnetic fields are fully coupled. The computational domain includes a layer of slag and a layer of liquid steel. A VOF approach is used for the interface tracking and a potential formulation is used for the electric and the magnetic field. It is shown that a complex interaction between the electromagnetic field and the phase distribution occurs. This interaction generates a strong 3D flows that cannot be predicted with conventional 2D models.

Introduction

In the near future, the steel industry will have to produce much larger ingots for larger parts with improved cleanliness levels and at very low segregation limits. For example the aviation industry and power supply industry are looking for larger diameters e.g. for bearings, plates, discs and shafts for turbines. Large number of publications can be found in the field of simulation of the ESR process, but almost all are performed in 2D [1-15]. Unfortunately simple models using rough 2D approximations cannot be used in large geometries where 3D effects are believed to be dominant. For fundamental and technical reasons it is then important to study how the droplets form and behave in the slag.

A 3D model has recently been built and applied to small geometries [16]. This model is now used to explore the droplet formation during the melting of an industrial scale electrode. During the process the solid electrode can develop a flat or a parabolic surface, here it is assumed flat. The process of phase change, melting and solidification are not taken into account. The electric current distribution is dynamically calculated from the transient phase distribution. Then the electromagnetic forces and the Joule heating are recalculated at each time step.

Numerical Model

The fluid calculation domain is a cylinder divided into 13.8 million volume elements (Figure 1). The mesh is refined at vicinity of all wall boundaries, especially near the electrode where a thin liquid film develops during the melting. The electrode has a radius of 21 cm. The container is initially filled with the quantity of liquid slag (10 cm high) and liquid steel (10 cm high). The interface between the air and the slag, known as the exposed slag surface, is modelled with a slipping fixed wall. Only the thermal and electric conductivity of the slag are temperature dependants, all others properties are considered as constant (Table I).

The electromagnetic field is solved on a cylindrical domain which is 30 cm high and 75 cm radius. It includes the fluid domain, the solid electrode (10 cm high), and a large surrounding void region (Figure 1). Inside the fluid region the electromagnetic field is resolved on the same mesh than the momentum field. Outside the fluid region much less variations of the electromagnetic field is expected, thus only 238 000 volume elements are used to mesh this outer domain. The electrode supplies a total DC current of I_0 = 13 000 Amperes.

Table I: Process parameters and averaged material properties used

Slag	
Density	2700 kg/m^3
Viscosity	0.0025 kg/m/s
Specific heat, liquid	1200 J/kg/K
Thermal expans. coefficient	1x 10^{-4} K^{-1}
Electric conductivity, 1000 K	1.0x10^1 (Ωm)$^{-1}$
Electric conductivity, 1870 K	1.2x10^2 (Ωm)$^{-1}$
Thermal conductivity, 2000 K	2.0 W/m/K
Thermal conductivity, 750 K	0.41 W/m/K
Steel	
Density	6850 kg/m^3
Viscosity	0.006 kg/m/s
Specific heat, liquid	750 J/kg/K
Thermal expan. coefficient	2.1x 10^{-5} K^{-1}
Electric conductivity	7.0x10^5 (Ωm)$^{-1}$
Thermal conductivity	26 W/m/K
Geometry	
Slag height, Metal height	100 mm
Electrode diameter	420 mm
Ingot diameter	600 mm

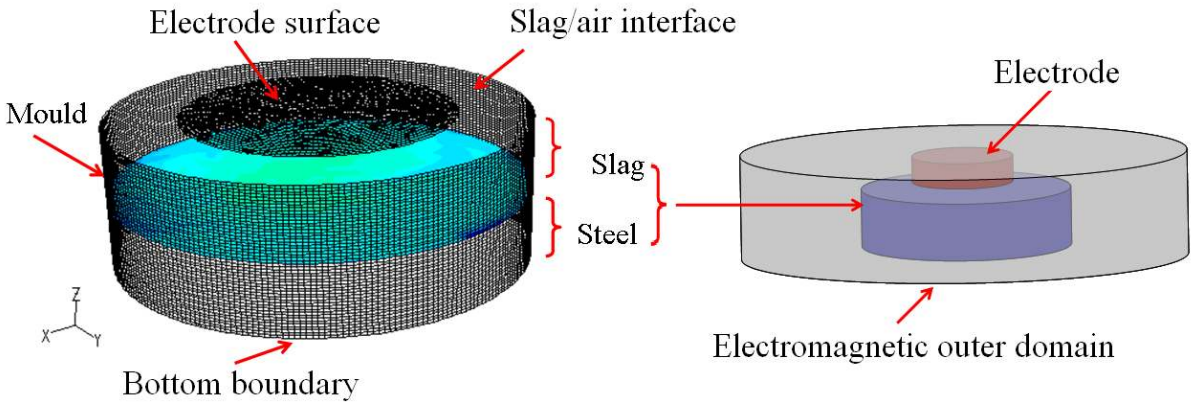

Figure 1: Calculation domain

The interface between the two phases is tracked with a geometric reconstruction VOF technique (Volume Of Fluid). A single set of momentum equations is shared by the fluids, and the volume fraction of each of the fluids in each computational cell is tracked throughout the domain. According to the local value of the volume fraction *f*, appropriate properties and variables are assigned to each control volume within the domain. The third order resolution MUSCL scheme is used for the space discretisation of all conservation equations. The second order Crank–Nicolson method is used for the discretisation in time resolution. The value of the interfacial tension between the slag and the metal is chosen to be equal to 1N/m.

Fluid Flow:
The motion of the slag and liquid steel is computed with the buoyant Navier-Stokes equations. The effect of the turbulence is estimated with the Smagorinsky LES model. The non-slip condition is applied at the mould wall, a slip condition is applied at the exposed slag surface. The slag/electrode surface and the bottom surface are modelled as velocity inlets with a fixed velocity (0.14 mm/s at the electrode, and 0.06mm/s at the bottom) corresponding to a melt rate of about 475 kg/hour.

Electromagnetics:
The electromagnetic field is solved by using the electric field φ and the magnetic potential vector $\vec{A}$ .Outside the liquid and the electrode domain no electric current is assumed to exist. A constant and uniform electric current flow is applied at the bottom boundary of the liquid domain, and a constant electric potential ($\varphi = 0$) is applied at the top of the solid electrode. The mould is assumed to be electrically insulated by the solidified slag layer, no current is allowed leave the domain through the lateral wall (mould). In the liquid the computed electromagnetic field is dynamically adjusted from the space distribution of the electric conductivity, which is in turn a function of the predicted phase distribution. It is then possible that the metal distribution in the fluid domain generates a non axisymmetric electric current flow.

Heat Transfer:
The energy equation is solved in the fluid domain. The Joule heating is taken as a source term in the energy equation. The temperature at the electrode/slag contact surface is fixed at the alloy liquidus temperature (1750 K). At the mould and at the bottom boundary, the temperature is fixed at the slag liquidus temperature (1650 K). The radiative emissivity of the slag surface is taken equal to 0.8.

Computation:
The time step is controlled by turbulence and the dynamic of the metal/slag interface through a chosen maximum courant number of 0.1. Depending on the droplet falling speed, the typical calculation time step lies in the range of 10^{-3}-10^{-5} second. The calculations, which for the present analysis lasted about 60 days, were performed with a supercomputer Intel Nehalem Cluster 2,93 GHz with 16 Cores.

Results and Discussion

To show the results we choose to plot the fields over the symmetry plane y = 0 and over the interface between the steel melt and the slag, which is defined as constant $f_1 = 0.5$ (Figures 2-4). In fact, the iso-volume fraction represents two surfaces, the first is the slag/pool interface, and the second is the surface enveloping the thin liquid film that develops just under the electrode. It is then clear that the iso-volume fraction surface changes constantly its shape with time, while the iso-y plane can be represented as a vertical curtain that hides what happens behind it. Between these two surfaces, the iso-volume fraction visualizes also the falling droplets.

Figure 2 represents the evolution of the electric current density during the formation and the departure of several droplets. To minimize the electric resistance, the electric current chooses in priority to travel through the liquid metal. Just under the electrode the typical liquid film thickness was found to be around 1-2 mm. The formation of a droplet starts by the thickening of the liquid film (5-7 mm) in a form of a bag. In Figure 2 a we can observe almost 20

positions from where the droplets can possibly depart. When the thickness of the liquid film bag exceeds 13 mm an elongated faucet forms. The electric current density increases strongly during the faucet formation. But when the departure of the first droplet occurs a slag gap forms between the drop and the remaining faucet, leading to a decrease in the current density. The electric current density decreases to lower values during the departure of smaller droplets (satellite droplets). The equivalent droplets diameter was found to be 10-15 mm for the largest, and 1-4 mm for the satellite droplets. During the fall, the large droplets flatten and develop a lentil or a crescent shape (Figure 2e). The depressions (with low electric current density) created by the impacts on the slag/pool interface can easily be observed in Figure 2 c-f).

Around the droplet being formed, the electric current density reaches values (10^7 A/m^2) much larger than those observed in the periphery of the electrode (10^5 A/m^2).

The velocity magnitude reaches a maximum of 0.65 m/s, however, this speed corresponds to the maximum speed of the falling droplets. The slag region affected by the droplets trajectory is strongly turbulent, from the 3 pictures given in Figure 3 it is not possible to draw a main 2D flow pattern. This is a strong indication that a strong momentum exchange occurs between the slag and the droplets. Outside the droplets falling region the main flow velocity rarely exceeds 0.18 m/s, but surprisingly the flow in the liquid melt was found to be as turbulent as in the liquid slag.

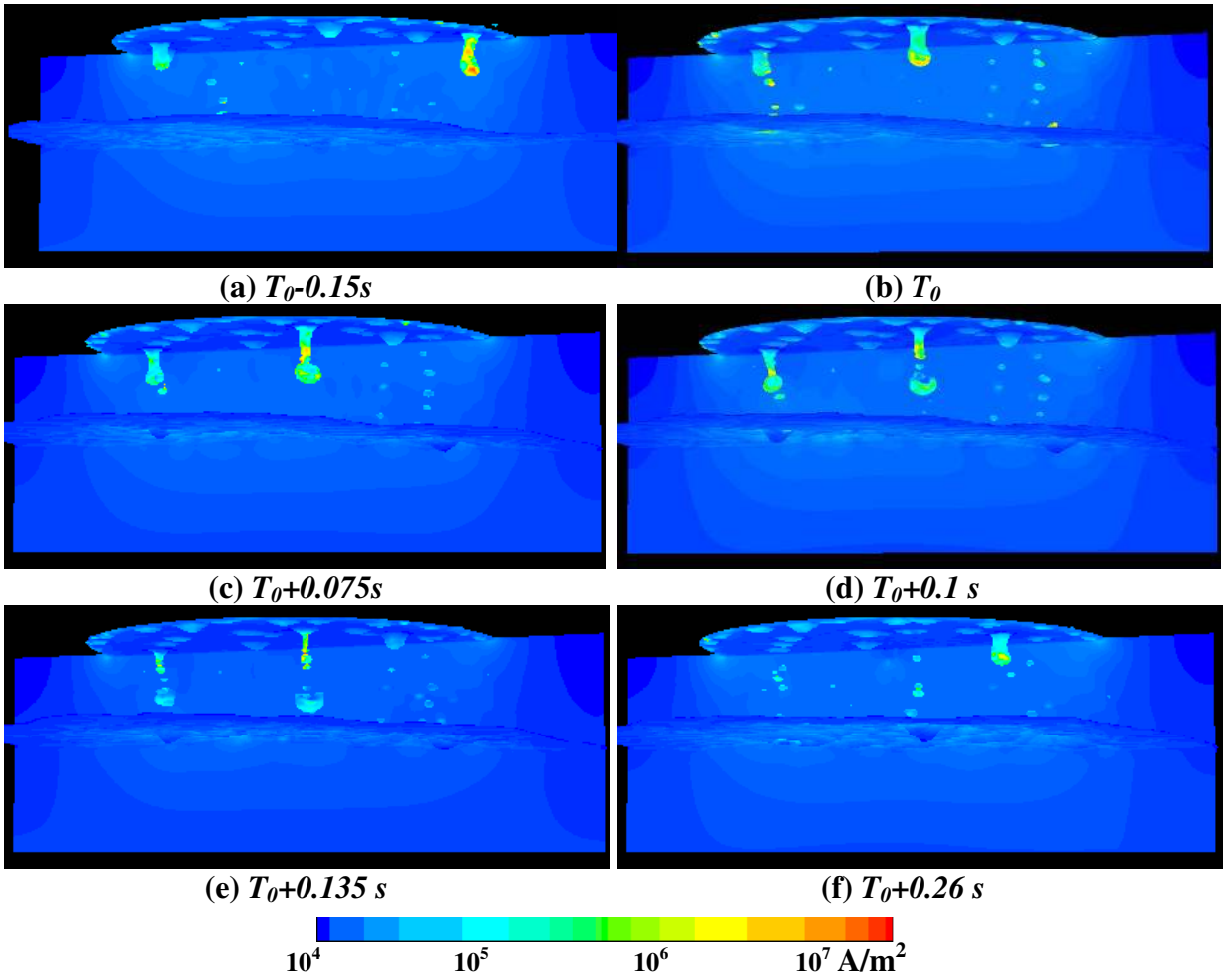

Figure 2: Electric current density

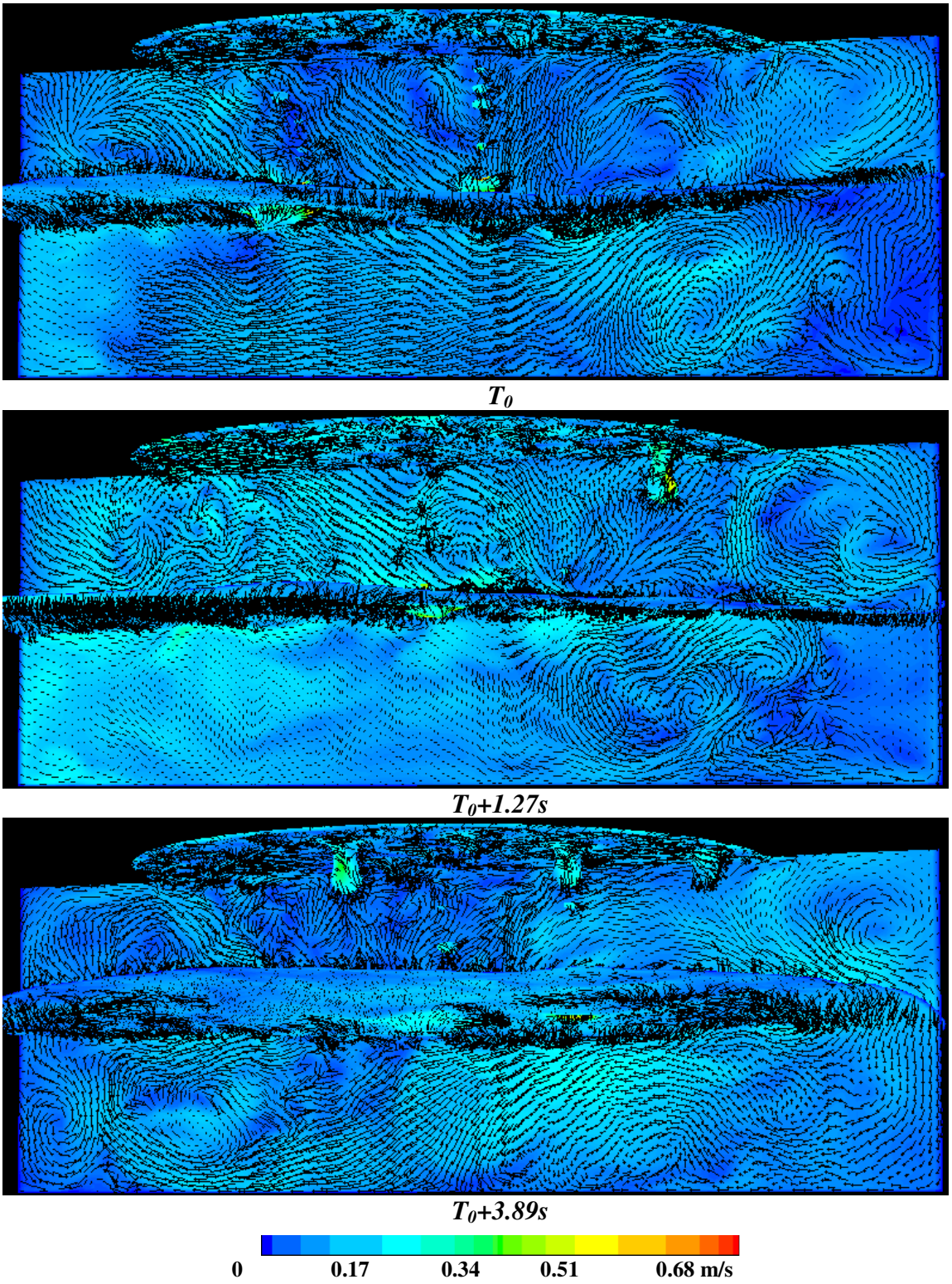

Figure 3: The flow direction vectors and velocity magnitude. The vectors have all the same length. Small apparent vectors are vectors that are meanly directed in the direction perpendicular to the vertical plane**.**

The movement of the liquid-pool interface is clearly observable in Figures 2-4. The maximum measured elevation of the interface is of about 3 cm. Its movements has a strong non axis-symmetric behaviour, resulting from MHD actions such those observed in

aluminium reduction cells [17-19]. The redistribution of the liquid generated by the interface movement within the cylindrical domain is the main source of this 3D flow behaviour. The flow generated by the droplets, due to the fall or due to the local deviation of electric current, is another source for three dimensionality of the flow. In the same time the falling droplets influence the dynamic of the interface through their momentum impacts, but also by their influence on the current distribution within the slag layer. The quantification of the 3D effects can be estimated by computing the ratio of the normal to the mean velocity over a centred vertical plane. This ratio must be small in order to be allowed to decompose the flow in a mean and a fluctuating (turbulent) part. It can be seen in Figure 4, that the level of turbulence is such that this ratio exceeds 50% over almost the entire plane. This indicates that the use of a steady RANS approach to model the present turbulent system cannot be justified.

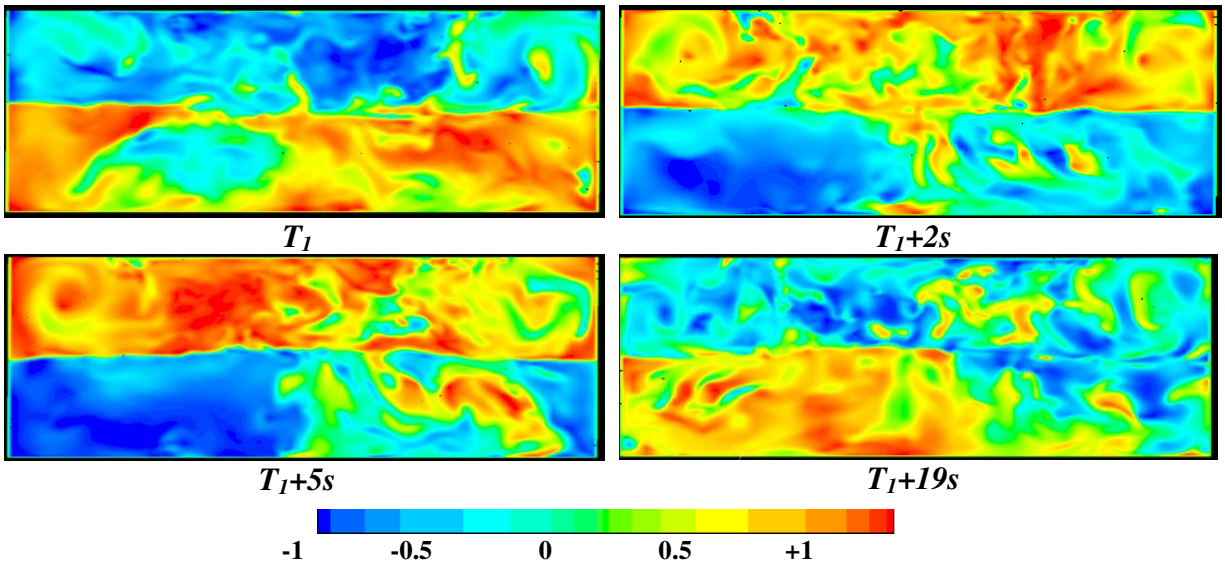

Figure 4: Ratio between normal to mean velocity over the vertical plane of y = 0.

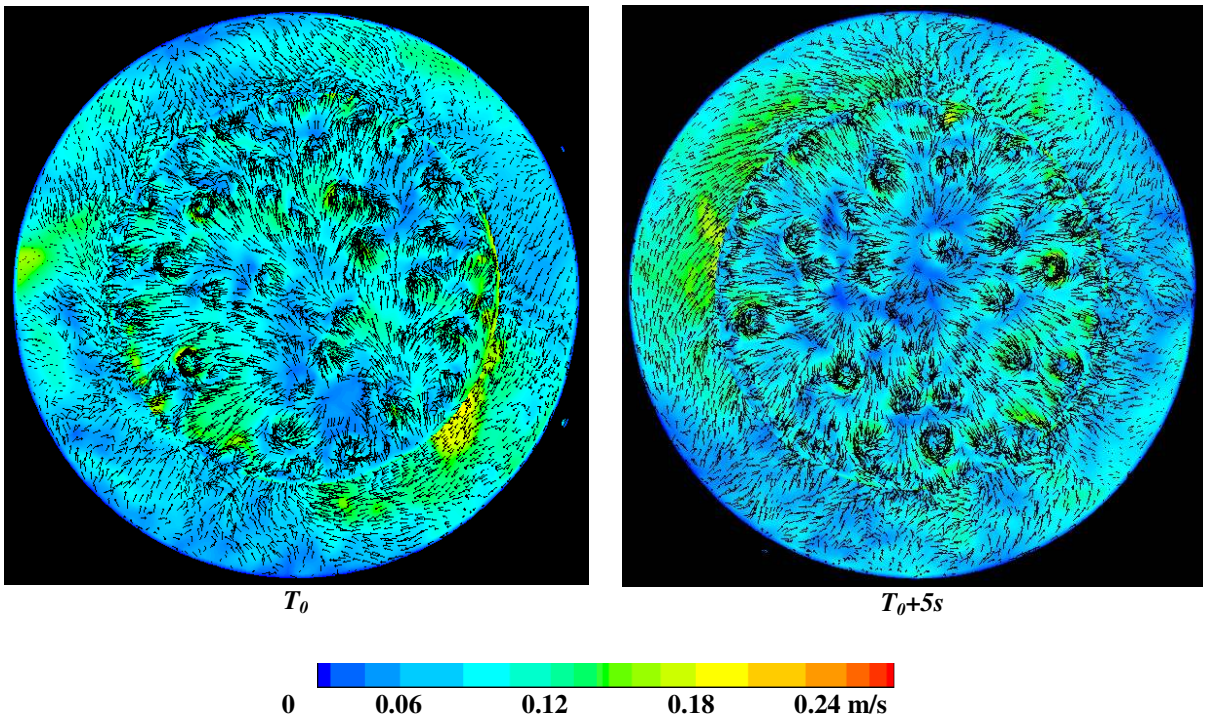

Figure 5: Velocity field over the exposed slag surface and at the first slag/metal interface under electrode (liquid metal film and droplet). The vectors have all the same length. Small

apparent vectors are vectors that are meanly directed in the vertical direction.

A view from the top (Figure 5) shows that the velocity over the slag surface is not uniformly radially oriented as would be expected from 2D simulations. In large region the velocity vectors have temporally a tangential orientation. It is also possible to observe area where the liquid is rising from the bulk. The flow just under the liquid film has a clear orientation, mainly radial. This orientation is due to the rise of the slag flow. The latest can be generated by thermal buoyancy, by the displacement generated by a group of falling droplets, or by a more complex mechanism that involves the slag/metal interface movement. Due to the accumulation of liquid metal, the positions of liquid metal bags from which a droplet can possibly depart can be clearly seen in Figure 5.

Conclusions

In the present work a 3D VOF model was coupled with a Magneto-hydrodynamic model to simulate the droplet formation during the melting of an electrode. The model can predict the electric and magnetic field distribution in function of the metallic distribution in the low electric conductivity slag. The model was applied to the melting of an industrial scale electrode assuming a constant melting rate and a constant imposed DC electric current intensity.

The results can be summarized with the following:

1) The droplets formation, departure, and movement in the slag disturb the distribution of the electric current density.
2) The droplets have diameters of about 1-15 mm. Due to drag and electromagnetic mechanisms, the droplets falling generate strong turbulences in the slag flow.
3) Due to MHD forces and to the droplets impacts, the slag/pool interface moves with a non axis-symmetric pattern which in turn generates a turbulent flow within the liquid pool

Three dimensional effects are found to be already dominant in this 60 cm diameter process, one can expects even stronger effects for diameters larger than 1 or 2 m. In this work a DC current was assumed, the application of an AC current would generate eddy currents which could perturb the droplets formation. For frequency of about 50 Hz a strong change in direction of the electric current would exists at the slag pool boundary, which can promote vortical movements of the slag metal interface. However most of the conclusions given here are believed to be still valid when an AC current is applied. In addition quasi DC field (~0.1-1Hz) are planed to be applied to future ESR remelting of very large ingots. Other simulations studying the influence of various current shape and frequency, the material properties, the possible presence of mould current, the influence of electrode penetration depth are planed.

Although computationally extremely expensive, three dimensional MHD simulations are rather necessary if we want to obtain fundamental knowledge of the process. The results can then be used to further develop or to tune the actual 2D models in order to give simultaneously fast and good results.

References

1. Choudhary M., Szekely J., *Metall. Trans. B*, vol. 11B, 1980, p. 439.
2. Dilawari A.H., Szekely J., *Metall. Trans. B*, vol. 8B, 1977, p. 227.
3. Choudhary M., Szekely J., *Ironmaking and Steelmaking*, vol. 5, 1981, p. 225.

4. Jardy A., Ablitzer D., Wadier J. F., *Metall. Trans.*, vol. 22B, 1991, p. 111.
5. Hernandez-Morales B., Mitchell A., *Ironmaking and Steelmaking*, vol. 26, 1999, p. 423.
6. Kelkar K.M., Mok J., Patankar S.V., Mitchell A., *Phys. IV France*, vol. 120, 2004, p. 421.
7. Patel A., *Proc. of Liquid Metal Proccessing and Casting,* ed. P. D. Lee, A. Mitchell, J. Bellot, and A. Jardy, 2003, p. 205-214.
8. Patel A., *Proc. Proc. of Liquid Metal Proccessing and Casting,*, ed. P. D. Lee et.al (SF2M, 2007), p.95-100.
9. Weber, V., Jardy, A.; Dussoubs, B., et al, *Metall. Trans. B,* vol. 40B, 2010, p.271-280
10. Kharicha A., Schützenhöfer W., Ludwig A., Tanzer R., Wu., *Steel Res. Int.*, vol.79 (8), 2008, p. 632-636.
11. Kharicha A., Schützenhöfer W., Ludwig A., Tanzer R.. Wu M., *Int. J. Cast Metals Res.*, vol. 22, 2009, p. 155-159.
12. Kharicha A., Schützenhöfer W., Ludwig A., Tanzer R., Wu M., *2nd Int. Conf. Simul. Model. Metallurgical Processes in Steelmaking (STEELSIM 2007)*, Graz, Austria, Sept. 12-14, 2007, ed. Ludwig A., Knittelfeld: Gutenberghaus Druck GmbH, p. 105-110
13. Kharicha A., Mackenbrock A., Ludwig A., Schützenhöfer W., Maronnier V., Wu M., Köser O., *Int. Sympo. Liquid metal Processing and casting (ICASP 2007)*, Sept. 2-5, 2007, Nancy, France, eds. Lee P.D., Mitchell A., Bellot J.P., Jardy A., p. 107-113.
14. Kharicha A., Ludwig A., Wu M., *Mater. Sci. Eng. A*, vol. 413, 2005, p. 129-134.
15. Kharicha A., Ludwig A., Tanzer R., Schützenhöfer W., *Mater. Sci. Forum*, vol. 649, 2010, p. 229-236.
16. Kharicha A., Ludwig A., *Int. Conf. on Multiphase Flows,* ICMF 2010, June 2010, Tampa, Florida.
17. ASneyd. D., *J. Fluid Mech.*, vol.156, p. 223–236, 1985.
18. Bojarevics V. & Romerio M., *Eur. J. Mech.* B, Vol 13, 1994, p 33–56.
19. Munger D., Vincent A, *Magnetohydrodynamics*, vol 42, 2006, p 417–425.